factors, barring significant crystal packing forces, etc., we are confident that our calculations accurately represent the conformational properties of polysilane and poly(dimethylsilylene).

(41) Natta, G.; Corradini, P.; Bassi, I. W. *Nuovo Cimento, Suppl.* **1960**, *15*, 68. See also ref 27.
(42) Atkins, E. D. T.; Keller, A.; Shapiro, J. S.; Lemstra, P. J. *Polymer* **1981**, *22*, 1161 and references therein.

Assessment of Long Branches in Free Radical Polyethylene: Correlation between the Melt and Solid States

Fadhel ben Cheick Larbi,[†] Marius Hert,[‡] Marie-France Grenier,[§] and Jacques Rault*[†]

Laboratoire de Physique des Solides, Bâtiment 510, Université de Paris-Sud, 91405 Orsay Cedex, France, CDF-Chimie, 62160 Bully les Mines, France, and Chimie Organique Physique, Université, 64000 Pau, France. *Received September 29, 1983*

ABSTRACT: A series of branched polyethylenes of the same apparent molecular weight have been characterized by gel permeation chromatography (GPC), viscometry, NMR, and SAXS. By use of these different techniques, the molecular weight distribution and the number of long branches have been determined. In these materials quenched from the melt, we show that the long period of the semicrystalline state and the dimensions of the coils in the melt before crystallization are correlated. These correlations permit verification of theories of Zimm and Stockmayer and Daoud and Joanny giving the conformations of the coils in the melt. Finally, we emphasize that the SAXS technique combined with GPC is an accurate method of assessment of the number of branches, comparable to the ^{13}C NMR technique and viscometry.

I. Introduction

In a series of papers it has been shown that in monodisperse fractions, mixture of fractions, and polydisperse polyethylene (PE), the quenched state and the melt state are correlated.[1-3] For these linear chains, the long period L of the semicrystalline state is a function of the weight average of the radius of gyration R_w. The relationship

$$L \cong R_w \sim \sum_i \omega_i M_i^{1/2} \tag{1a}$$

where ω_i is the mass concentration of chains of molecular weight M_i and has been verified for polyethylene and poly(ethylene terephthalate).[4]

In branched polymers, the dimensions of the coils vary with the molecular weight M and with the number of branches N_b per chain. These dimensions have been calculated by Zimm and Stockmayer[5] (ZS) and more recently by Daoud and Joanny[6] (DJ). Up to now neither the dimensions of the chains in the liquid state nor the long period in the solid state has been systematically studied for these randomly branched materials. By comparison with relation 1a we expect a long period dependence of the form

$$L \sim R \sim f(M)g(N_b) \tag{1b}$$

where $g(N_b)$ is a decreasing function of N_b. A knowledge of the functions f and g and a measurement of R or L would give an estimate of the number of branches N_b, if the molecular weight distribution is known.

The aim of this paper is to compare the assessment of long branches in radical PE by the three following methods coupled with gel permeation chromatography (GPC) on a series of well-defined high-pressure PE's: (a) viscometry, (b) NMR, and (c) small-angle X-ray scattering (SAXS) in the semicrystalline state obtained by quenching the melt.

The assessment of branching by methods a and b has been studied by several authors.[7-15,22] The last method, which is new, is based on the correlations existing between the solid and melt states of branched polymers expressed by relation 1b. Finally, we discuss our results in light of the scaling theory of Daoud and Joanny.

II. Characterization of Polyethylene Samples

1. GPC and Viscosity Measurements. We give in Table I the characteristics of branched (B) and linear (L) PE samples. For branched PE the GPC chromatogram at 135 °C in trichlorobenzene (TCB) permits us to define the apparent average molecular weights M_n* and M_w*, which are the number- and weight-average molecular weights of the equivalent linear PE having the same chromatogram. Samples B_1-B_8 have nearly the same chromatogram and, therefore, the same apparent molecular weight distribution (M_n* ~ 18 000, M_w* = 120 000).

Linear samples L_1-L_3 have been studied in ref 2 and 3. Sample L_1 is a mixture of equal weights of two monodisperse fractions of molecular weight 10 000 and 260 000. Samples L_2 and L_3 are two Pennings fractions.[3] L_1 and L_2 have different molecular weight distributions but the same weight- and number-average molecular weights as the apparent molecular weight of the branched PE samples B_1-B_8 (Figure 1).

Sample L_4 is a polydisperse, high-density commercial product (Manolene 6050). The indices of branching, b, of the materials have been determined from GPC and intrinsic viscosity measurements. Following the procedure given by Prechner et al.,[7] b is defined as the ratio of the intrinsic viscosity $[\eta]_l$* of the linear PE to the intrinsic viscosity of $[\eta]_b$, the branched PE having the same elution volume:

$$b = [\eta]_l^*/[\eta]_b \tag{2}$$

The parameter β can be calculated for each fraction; in Table I b is an average value, $[\eta]_l$* and $[\eta]_b$ being the weight average of the intrinsic viscosity of the linear and branched polymer, respectively.

[†] Université de Paris-Sud.
[‡] CDF-Chimie.
[§] Chimie Organique Physique, Université.

0024-9297/85/2218-0164$01.50/0

Table I
Characteristics of Branched (B) and Linear (L) Polyethylene Samples

samples	L, Å			$10^{-3}M_w$*	$10^{-3}M_n$*	b
	quenched	cooled 10 °C/min	cooled 3 °C/min			
B_1	191	218	237	123	18.5	1.55
B_2	207	227	234	105	18.8	1.58
B_3	191	228	232	123	19.4	1.60
B_4	188	219	234	107	17.2	1.64
B_5	189	219	232	119	18.0	1.70
B_6	183	214	236	132	18.5	1.75
B_7	175	214	230	127	12.0	2.10
B_8	168	210	227	156	17.0	2.21
B_0	170	220	240	101	16	1.3
L_1 (0.5 M_1 + 0.5 M_2)	235	320	400	135	19.3	1
L_2 (Pennings)	227	350	420	138	21.6	1
L_3 (Pennings)	200	300	380	90	15.7	1
L_4	260	360	380	219	30	1

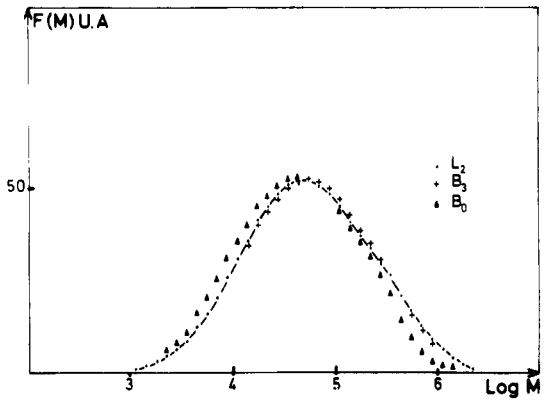

Figure 1. Chromatograms of two branched PE (B_0 and B_3) and a linear PE (L_2). The samples B_1–B_8 have the same chromatograms as the linear L_2, indicating therefore that they have the same apparent molecular weight distribution.

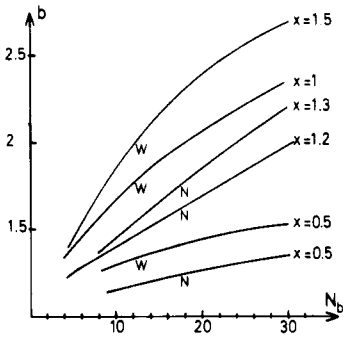

Figure 2. Index of branching b measured by viscometry as a function of the number of long branches N_b, in random branched polymers. The number of branched N_b is calculated from the theory of Zimm and Stockmayer (relations 8 and 9 giving the structure factors g_n and g_w) and from the empirical relation $g' = (1/b)^{1.69} = g_{n,w}{}^x$ (relations 6 and 10).

The intrinsic viscosity $[\eta]_l$* of the equivalent linear polymer is calculated by the Mark–Houwink relation

$$[\eta]_l^* = KM_l^{*a} \tag{3}$$

where $K = 5.16 \times 10^{-4}$ dL g^{-1} and $a = 0.69$ for a dilute solution in TCB at 135 °C.[22]

The equivalent mass M_l* of the linear chain is given by the hydrodynamic volume V:

$$V = [\eta]_b M_b = [\eta]_l^* M^* \tag{4}$$

The molecular weight of the branched chain is then

$$M_b = M_l^* b \tag{5}$$

Branched polymers are often characterized by the ratio g' of the intrinsic viscosities of the branched and linear chains having the same molecular weight.

$$g' = [\eta]_b/[\eta]_l \tag{6}$$

Combining relations 2–6, the relationship between the ratio g' and the index of branching b is found to be

$$g' = [1/b]^{1+a} \tag{7}$$

Several authors[8-12,24-31] have attempted to correlate these viscosity parameters with the number of branches per chain, N_b, and to the structure parameter g, which is defined as the ratio of the square of the dimensions of branched and linear chains having the same molecular weight:

$$g = R_b{}^2/R_l{}^2 \tag{8}$$

The structure parameter g can be calculated if some assumptions are made for well-defined branch geometries. In the unperturbed case, for fractionated and for unfractionated materials, these parameters have been calculated by Zimm and Stockmayer,[5] in cases of a random distribution of the branches:

$$g = g_n = [(1 + N_b/7)^{1/2} + 4N_b/9\pi]^{-1/2} \tag{9}$$

$$g = g_w = \frac{6}{N_b}\left[\frac{1}{2}\left(\frac{2+N_b}{N_b}\right)^{1/2} \log \frac{(2+N_b)^{1/2} + N_b{}^{1/2}}{(2+N_b)^{1/2} - N_b{}^{1/2}} - 1\right] \tag{10}$$

In the first case N_b is the average number of branches per molecule and in the second case the weight average. These relationships are not valid for star chains.

As noted by Small,[9] for branched polymers there is no unique relationship between the viscosity parameter g' and the structure parameter g. This is not surprising in view of the complexities of the branched structures.

Several authors have attempted to apply the relation

$$g' = g^x \tag{11}$$

to polyethylene, with $x = 0.5$,[9] 1,[10] and 1.3.[11] Combining 5, 9 or 10, and 11, the relationships between b and N_b are found. Figure 2 shows that for $1.5 < b < 2$, the relationship between b and N_b can be considered linear. For example, if we put $g = g_w$ (eq 10) and $x = 1$ and 1.5 in eq 11, we obtain the approximate relation 12 in the domain $1.3 < b < 1.9$:

$$b = 1.1 + 0.05N_b \quad (x = 1) \tag{12a}$$

$$b = 1.1 + 0.08N_b \quad (x = 1.5) \tag{12b}$$

Table II
Number of Branches (N_b) per 1000 Carbons in Polyethylene

	sample			
	B_0	B_3	B_6	B_8
nature				
CH_3 (λ_0)	13–15	16–17	19–20	22–23
C_2H_5 (λ_1)		4	4	
C_3H_7 (λ_2)	1–2	<2	1–2	2
C_4H_9 (λ_3)	8	5	6	9
C_6H_{13} (λ_5)	4	2	3	5
λ_L	2–3	4–5	5–6	7–8
N_b (NMR)	3–4.5	9–11	11.5–13.8	19–21
ZS				
$N_b(x = 1)$	4	8.6	11.6	25
$N_b(x = 1.5)$	3.3	6.5	8.5	16
$N_b(x = 1.7)$	3	4	5	7
b	1.33	1.6	1.75	2.21

In Table II, values of N_b obtained for $x = 1.0$, 1.5, and 1.7 are compared.

In conclusion, from the measurements of the index of branching b by coupling GPC and intrinsic viscosity measurements and from the theory of Zimm and Stockmayer it is possible to determine the average number of branches N_b per molecule. However, it must be emphasized that this number depends on certain assumptions about the structure of the chain via the structure parameter g and the parameter x which appears in the relationship between the structure parameter and the viscosity parameter.

For PE the most reliable value of x is 1.0 ± 0.3, according to Small.[9] The different values of x found in the literature[9,10,12,25] very likely come from the difference in the structure of the branched chains. The relation $g' = g^x$ is an empirical relation which has no physical basis. It should be noted that in the limiting cases of star chains and combs x is 0.5 and 1.5, respectively. Hert and Strazielle[25] have found by light scattering that the exponent x is somewhat dependent on the type of synthesis of the PE and on the molecular weight. For high molecular weight materials they found $x \sim 0.9$. We show in the next paragraph that in our materials the exponent has this same value, and therefore we conclude that the structure of the branched chains in our materials and in the materials analyzed by Hert and Strazielle are intermediate between stars and combs.

It is important to note that the value of g given by (6) and 11) with $x = 1$ decreases first rapidly with the branching index and with N_b and then slowly for $b > 1.3$.

In the domain $1.5 < b < 2$, the relationship between g and b has the linear form

$$g = 0.9 - 0.4(b - 1)$$

thus

$$R_b = R_l^0[1 - 0.20(b - 1)] \tag{13}$$

where R_l^0 is a constant different from R_l, the radius of gyration of the linear chain having the same molecular weight. We shall see in section II.3 that the long period in the semicrystalline state obeys a similar equation.

2. NMR. The ^{13}C NMR spectra of the polymers were recorded by using 10-mm sample tubes at 62.89 MHz and 120 °C in a Bruker WM 250 spectrometer provided with an Aspect 2000 computer and an interactive disk unit. The polymers were dissolved in a mixture of 80% (v/v) 1,2-dichlorobenzene and 20% (v/v) 1,2-dideuteriotetrachloroethane. Sample concentration was 10% (w/v).

The instrumental conditions were as follows: pulse angle, 90° (25 μs); pulse delay, 135 s; sweep width, 3800 Hz; digital resolution, 0.233 Hz/point (0.003 ppm/point); number of transitions, 200. The pulse spacings are considered adequate for qualitative measurements. The inverse gated decoupling method was employed to suppress the NOE.

From the analysis of the NMR spectra, one can evaluate the concentration of seven types of branches: ethyl, butyl, pentyl, hexyl, 2-ethylhexyl, 1,3 paired ethyl and long branches having more than eight methylene groups.[13-18] To assess correctly the NMR peaks, the spectra of the low-density PE have been compared to those of a series of PE models compounds having well-characterized short branches.[18-21] Nearly all the peaks of the different PE have been identified. In Figure 3, the ^{13}C spectrum of sample B_3 is given as an example. The number of branches is deduced from the peak areas, by averaging 10 integrations; this technique, described by Bovey et al.[13] and Randall,[15] leads to an accuracy of the order of 1% on the number of branches.

The number per 1000 carbons of short branches having i CH_2 groups is denoted λ_i and is reported in Table II. In all samples the number of butyl branches λ_3 is important. Roedel[22] suggested that these branches are created by the mechanism of "back-biting". The total number of the more complex branches 2-ethylhexyl and 1,3 paired ethyl has been evaluated. Those branches which lead to characterized peaks as seen in Figure 1 have been predicted by Willbourn.[23]

The number of long chains per 1000 carbons λ_L has been evaluated directly by measurements of the area of the peak C^3L indicated in Figure 3; it should be noted that this number is equal to the difference

$$\lambda_L = \lambda_0 - \sum_i \lambda_i \tag{14a}$$

where λ_0 is the number of CH_3 group (chain ends) per 1000 carbons.

This indicates that the numbers of short chains other than those reported in Table II are negligible. This leads to the important conclusion that if, during the synthesis, a branch of 8 carbons is created, the probabilities of growth of the two chain ends separated by 16 carbon atoms are equal and that the notion of backbone chain (or main chain) is no longer relevant. It is therefore more appropriate to define λ_L as the number of long-chain branch points per 1000 carbons. From the measurement of λ_L, it is possible to calculate the number of LCB per chain. According to Foster et al.,[24] the number and weight averages (N_{bn}, N_{bw}) of the number of LCB are respectively

$$N_{bn} = \frac{M_n}{14000}\lambda_{Ln} \tag{14b}$$

$$N_{bw} = \frac{M_n}{14000}\lambda_{Lw} \tag{14c}$$

where λ_{Ln} and λ_{Lw} are the number- and weight-average values of the branching frequency per 1000 carbons. It must be noted that these two averages are functions of the number-average molecular weight and not of the weight-average molecular weight.[24]

In Table II, we give the value of N_b deduced from the above relations, the value of λ_{Ln} being that obtained by NMR (λ_L). Table II and Figure 4 show that the best agreement between the value of N_b determined by NMR and by viscometry, using the ZS theory, is obtained for $x = 1$ and for $x = 1.5$ (dashed line in Figure 4). The values of N_b determined by the both methods differ by 20%.

3. Long Periods Determined by SAXS. The long period L of the quenched materials has been determined

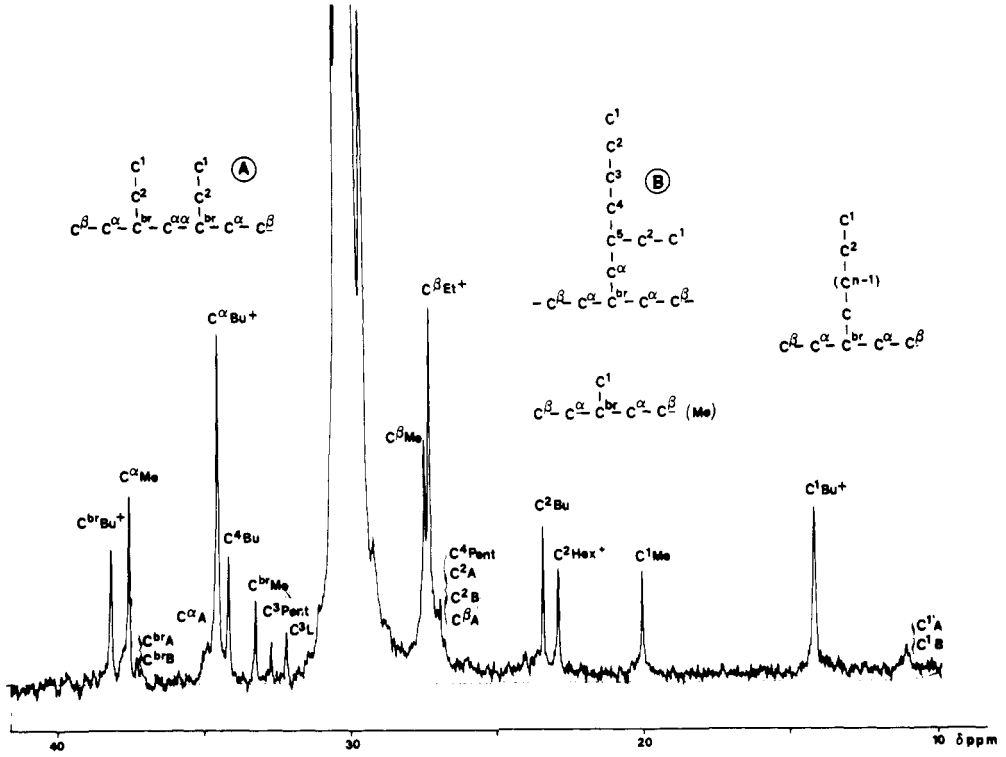

Figure 3. ^{13}C NMR spectrum of sample B_3 at 62.89 MHz and at 120 °C. The number of long branches having more than eight carbons is evaluated directly by measurements of the area of the peak C^3L.

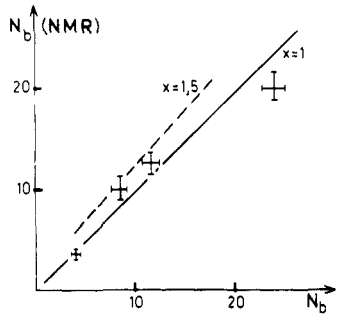

Figure 4. Comparison between the numbers N_b of long branches in radical PE evaluated by ^{13}C NMR and by viscometry. In the last method, the relation $g' = g_w^x$ is assumed to hold, g' is the viscosity parameter given by eq 6, and g_w is given by the ZS theory (eq 9).

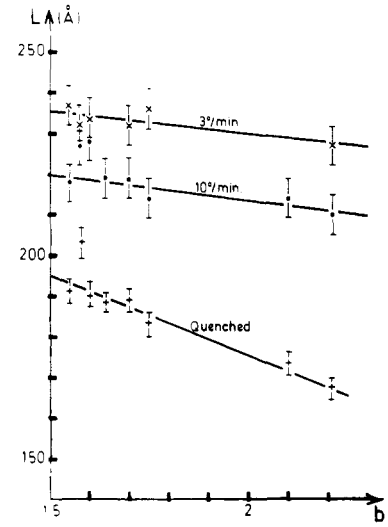

Figure 5. Long period of branched PE samples having the same chromatogram (the same apparent molecular weight distribution) as a function of the index of branching.

by the application of the Bragg law to the intensity maximum of the small-angle X-ray scattering (SAXS). The experimental arrangement has been described in ref 1 and 2. The relative width of the Bragg peak is the same for all the samples, and the precision of the location of the maximum intensity in the SAXS gives a precision for the long period of ±3 Å.

In Table I are given the values of the long periods for samples cooled at 10 and 3 °C min^{-1}. In Figure 5, the long periods are reported as functions of the index of branching b and of the cooling rate.

From these results, several conclusions can be drawn:

(a) For branched PE having the same apparent molecular weight, the long period is a decreasing function of the branching index following the relation

$$L_b = L_1^0[1 - \alpha(b - 1)] \quad (15)$$

For quenched PE, the ordinate at the origin $b = 1$ is $L_1^0 = 215$ Å, a value which is less than the long period, 230 Å, of quenched linear PE of the same apparent molecular weights M_n and M_w (samples L_1 and L_2). Samples B_0 and L_3 have nearly the same apparent molecular weight; the long periods are 170 and 200 Å, respectively.

(b) In slow-cooled materials, the long period is independent of branching and the ordinate at the origin $b = 1$ of the curve $L = f(b)$ is much less than the value of the long period of the linear polymer. The difference between the long periods of linear and branched PE of the same molecular weight crystallized at low cooling rate is explained by the fact that branches hinder the thickening process during crystallization.

Crystallization can be visualized as a two-stage process. During the first stage, only small segments crystallize involving small rearrangements of the chains. During this process there is no change in the radius of gyration of the coils. During the second stage, annealing leads to perfection of the crystalline lamellae and thickening. This latter process depends on the mobility of the chain in the crystalline phase and in the melt phase. For chains having

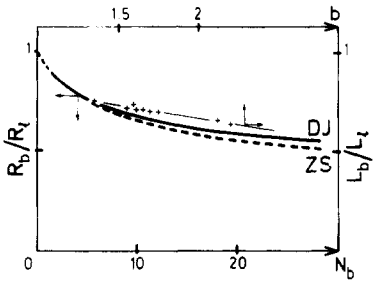

Figure 6. Correlation between the solid and melt states of branched PE: ratios R_b/R_l of the radius of gyration of the branched and linear coils having the same molecular weight as a function of the number of branches N_b (ZS, Zimm and Stockmayer theory eq 8 giving g_w; DJ, Daoud and Joanny eq 21 giving g_m); ratio L_b/L_l of the long period of the branched and linear materials, having the same molecular weight and quenched to room temperature, as a function of the viscosity index. The correspondence between the experimental points determined by SAXS and the theoretical curves gives the relationship between b and N_b (eq 11 and 17).

bulky groups, groups having hydrogen bonding or long branches, the mobility is very low and therefore the dependence of the long period on temperature of crystallization or cooling rate is very weak.[26]

(c) The long period of linear PE is greater than that of branched PE having the same total molecular weights M_n and M_w. Applying relation 5, the M_n and M_w values of sample B_0 are found to be 21 000 and 134 000, respectively, very similar to those of the linear sample L_2. The long periods of these branched and linear materials quenched to room temperature are 170 and 227 Å, respectively.

In the same way, samples B_1–B_8 and L_4 have the same total molecular weights (M_n = 30 000, M_w = 200 000). The long periods of the branched polymers vary from 200 to 170 Å with b, and that of the linear polymer is 260 Å.

The long period L_b of the branched polymers for $1.3 < b < 2.2$ can be put in the linear form

$$L_b = L_l^0(1 - 0.13(b - 1)) \tag{16}$$

which is very similar to relation 13 giving the radius of gyration of the coils in the melt state according to the ZS theory.

From these findings one may conclude that in branched polymers, as in linear polymers, the semicrystalline and melt states are correlated. These correlations are illustrated in Figure 6, where the variation of the ratio of the long periods L_b/L_l with the index of branching b is compared to the variation of the ratio of the radius of gyration R_b/R_l with the number of branches N_b, R_l and L_l being the radius of gyration and the long period of the linear PE having the same total molecular weights M_n and M_w (see eq 5). In this diagram the correspondence between b and N_b is given by relation 12a, which is verified by NMR measurements. As is shown in this figure, the experimental points do not fit exactly on the theoretical curve of Zimm and Stockmayer (dashed line calculated from relations 6, 9, and 10 with $x = 1$).

A good fit between L_b/L_l and R_b/R_l is obtained, if the relationship between b and N_b is

$$b = 1 + 0.083N_b \tag{17}$$

instead of relation 12a. Relation 17 is very similar to relation 12b obtained by the ZS theory with the parameter $x = 1.5$.

In conclusion, the estimate of the number of long branches can be obtained by the SAXS technique coupled with GPC by comparing the values of L_b/L_l to R_b/R_l. This number is about 20% smaller than that obtained by other techniques such as GPC and viscometry and by NMR.

Table III
Comparison of Structure Factors to Structure Parameters and the Viscosity Parameter

	b			
	1.33	1.6	1.75	2.2
N_b (NMR)	4	9	12	20
DJ				
g_s	0.758	0.644	0.60	0.549
g_θ	0.794	0.693	0.66	0.606
g_m	0.63	0.48	0.43	0.37
g'	0.618	0.45	0.39	0.26
g_m/g'	1.2	1.3	1.39	1.48
g_s/g'	1.2	1.4	1.5	2
ZS				
g_w	0.64	0.42	0.36	0.29
g_n	0.77	0.62	0.56	0.45
g_{SAXS}	0.63	0.54	0.49	0.41
g_m/g_{SAXS}	1	0.9	0.87	0.9
g_s/g_{SAXS}	1.2	1.119	1.22	1.34

From the measure of L_b and L_l we can define the structure parameter g_{SAXS}:

$$g_{SAXS} = L_b^2/L_l^2 \tag{18}$$

We will compare this parameter to the other structure parameters in the following section.

III. Discussion

As noted by several authors,[9,24,25] the GPC and intrinsic viscosity are measured in good solvent and the ZS theory applies to unperturbed chains. In good solvents the polymer chains are expanded, and moreover the expansion coefficient is dependent on the number of branches.[27] This fact is not taken into account in the determination of N_b by coupled GPC and intrinsic viscosity methods. Therefore, it does not seem appropriate to compare the dimensions of the coils measured in good solvent to the theoretical unperturbed dimensions. It is necessary to compare the structure parameters g for the different situations represented by dilute solutions and the melt.

Daoud and Joanny[6] have discussed the theoretical conformations of random chains in various types of solutions and in the melt. The radii of gyration in good and Θ solvents and in the melt are respectively for $N_b > 1$

$$\begin{aligned} R_{gs} &\sim N^{5/10}(N_b/N)^{-1/10} && \text{good solvent} \\ R_\theta &\sim N^{7/16}(N_b/N)^{-1/12} && \theta \text{ solvent} \\ R_m &\sim N^{1/3}(N_b/N)^{-1/6} && \text{melt} \end{aligned} \tag{19}$$

These relations are deduced from scaling arguments. For small number of branches $N_b \sim 1$, one recovers the well-known power laws of linear chains:

$$\begin{aligned} R_{gs} &\sim N^{3/5} \\ R_\theta &\sim N^{1/2} \\ R_m &\sim N^{1/2} \end{aligned} \tag{20}$$

We define for these systems structure factors g_s, g_θ, and g_m, which tend to unity when the number of branches $N_b \sim 1$

$$\begin{aligned} g_s &= N_b^{-1/5} \\ g_\theta &= N_b^{-1/6} \\ g_m &= N_b^{-1/3} \end{aligned} \tag{21}$$

We have compared these values in Table III to the values

of the various structure parameters g_n, g_w, and g_{SAXS} and to the viscosity parameter g' for samples B_0, B_3, B_6, and B_8. The number N_b of long branches is deduced from NMR measurements. In Figure 6 are plotted the two curves $g_m^{1/2}$ and $g_w^{1/2}$ as function of N_b deduced from the DJ and ZS theories. It is to be noted that the ZS theory applies only to chains with a small number of branches and that the DJ theory applies to chains having a large number of branches. These two theories lead to comparable structure parameters, g_m and g_w. From Table III and Figure 6, we conclude that

$$g' = g_w \cong g_m = g_{SAXS} \tag{22}$$

The ratios g_s/g_{SAXS} and g_m/g_{SAXS} are, respectively, equal to 1.2 and 0.9 and do not vary with the number of branches. In conclusion, the parameter g_{SAXS} is a good parameter which characterizes the structure of the branched chains in the molten state.

As the measure of g' is done in good solvent, we would expect that $g' = g_s$. In fact, as shown by Table II, one has the linear relationship

$$g_s = g'(1 + 0.05N_b)$$

It is very astonishing that the difference between g' and g_s (and g_θ) increases when the number of branches increases. This difference would be due to two different causes.

(a) The structure factor g_s is not strictly equal to the structure parameters R_b^2/R_l^2; the coefficients in relations 19 and 20 are unknown and the scaling form of these relations apply for long chains and many random branches.

(b) The parameter g' is measured in good solvent; the viscosity is according to several authors[7-9,31]

$$[\eta] = \phi[R^2]^{3/2}/M \tag{23}$$

The Flory constant ϕ varies with the quality of the solvent, that is to say with the expansion of the coils. In branched polymers it has been shown by Candau et al.[27] that the expansion was a complex function of the branching. The constant ϕ in branch polymers would be dependent on the structure of the chains.[31]

For chains having small number of branches and near the Θ conditions, one would assume that the variation of ϕ with N_b is constant, and in that case one gets the relations

$$g' = g_s^{3/2} \tag{24}$$

$$g_s = g_m^{3/5} \tag{25}$$

and if one assumes that the structure factors defined by relation 21 are equal to R_b^2/R_l^2 one would get

$$g' = g_m^{9/10} = g_\theta^{1.8} \tag{26}$$

that is to say

$$g' = g_m \tag{27}$$

In Table III on remarks that the ratio g'/g_m is varying from 1.2 to 1.4 when the number of branches increases from 4 to 20; simultaneously the ratio $g_s^{3/2}/g'$ increases from 1 to 1.5. For large number of branches $N_b > 10$, one concludes that relations 24–27 are no longer valid and that the Flory constant ϕ varies with N_b.

This feature has been pointed out by several authors[9,31] and it is the reason why it is interesting to characterize the branched chains by geometrical parameters like g_m and g_{SAXS}, which do not depend on the properties of the solvent.

IV. Conclusion

For a series of branched PE characterized by GPC, viscosity, and ^{13}C NMR, we have shown by the SAXS technique that the solid state and the melt state are correlated. This is a general law observed in several semicrystalline polymers. The long period and the radius of gyration vary in the same way with the molecular weight and the number of long branches. This is illustrated in Figure 6, which gives the variation of ratio of the long periods and dimensions of the coils of the branched and linear chains. The identity $L_b/L_l = R_b/R_l$ leads to an assessment of the number N_b of long branches. The values of the ratio of the coil dimensions of the branched and linear chains have been calculated by the theories of Zimm and Stockmayer and of Daoud and Joanny which rest on different assumptions; these two theories applying to chains with, respectively, small and large number of branches give the same results in the studied domain where $5 < N_b < 20$.

The number of long branches deduced from SAXS measurements and application of the ZS or DJ theories is found to be about 20% smaller than that measured by NMR or viscosity measurements. Considering that the accuracy of the measurement of N_b by the various techniques is of the order 10–20%, we conclude that this constitutes good agreement between these three methods. We think that it would be very interesting to measure directly the ratio R_b/R_l in the melt state to compare to the theoretical values deduced from the ZS and DJ theories and to compare to the values L_b/L_l determined by SAXS.

Acknowledgment. We are greatly indebted to the DGRST and the CNRS for financial support. We thank Dr. M. Daoud for his remarks and Dr. Strazielle for stimulating discussion.

Registry No. PE (homopolymer), 9002-88-4.

References and Notes

(1) Robelin, E.; Rousseaux, F.; Lemonnier, M.; Rault, J. *J. Phys. (Orsay, Fr.)* **1980**, *41*, 1469.
(2) Rault, J.; Robelin, E. *J. Phys. (Orsay, Fr.)* **1982**, *43*, 1437.
(3) Hert, M.; Rault, J.; Robelin, E. *Makromol. Chem.* **1983**, *184*, 225.
(4) Robelin, E.; Perez, G.; Rault, J. *J. Macrom. Sci., Phys.* **1983**, *B22*, 575.
(5) Zimm, B.; Stockmayer, W. H. *J. Chem. Phys.* **1949**, *17*, 1301.
(6) Daoud, M.; Joanny, J. F. *J. Phys. (Orsay, Fr.)* **1981**, *42*, 1359.
(7) Prechner, H.; Panaras, R.; Benoit, H. *Makromol. Chem.* **1972**, *156*, 39.
(8) Constantin, D. *Eur. Polym. J.* **1977**, *13*, 907.
(9) Small, P. A. *Adv. Polym. Sci.* **1975**, *18*, 1.
(10) Otocka, E.; Roe, R. J.; Hellman, M.; Muglia, P. *Macromolecules* **1971**, *4*, 507.
(11) Hama, T.; Yamagucki, K.; Suzuki, T. *Makromol. Chem.* **1972**, *155*, 283.
(12) Völker, H.; Luig, F. *Angew. Makromol. Chem.* **1970**, *12*, 43.
(13) Bovey, F. A.; Schilling, F. C.; Starnes, W. H., Jr. *Polym. Prepr., Am. Chem. Soc., Div. Polym. Chem.* **1979**, 160. Dorman, P. E.; Otocka, E. P.; Bovey, F. A. *Macromolecules* **1972**, *5* (5), 574. Bovey, F. A.; Schilling, F. C.; McCrackin, F. L.; Wagner, H. L. *Macromolecules* **1976**, *9* (1), 76. Cudby, M. E. A.; Bunn, A. *Polymer* **1976**, *17*, 345.
(14) Dichter, J. J.; Mandelkern, L. *J. Polym. Sci., Polym. Phys. Ed.* **1980**, *18*, 1955. Axelson, D. E.; Mandelkern, L.; Levy, G. C. *Macromolecules* **1977**, *10* (3), 557; **1979**, *12* (1), 41.
(15) Randall, J. C. *J. Polym. Sci., Polym. Phys. Ed.* **1973**, *11*, 275; **1975**, *13*, 901.
(16) Hoffman, W. D.; Eckardt, G.; Brauer, E.; Keller, F. *Acta Polym.* **1980**, *31* (4), 233.
(17) Grenier-Loustalot, M. F. *J. Polym. Sci., Polym. Chem. Ed.* **1983**, *26*, 83. Freche, P.; Grenier-Loustalot, M. F. *Eur. Polym. J.* **1984**, *20*, 84.
(18) Freche, P.; Gascoin, A.; Grenier-Loustalot, M. F.; Metras, F. *Makromol. Chem.* **1981**, *182*, 2305.
(19) Freche, P.; Gascoin, A.; Grenier-Loustalot, M. F. *Makromol. Chem.* **1982**, *183*, 2305.

(20) Freche, P.; Grenier-Loustalot, M. F. *J. Polym. Sci., Polym. Chem. Ed.* **1983**, *21*, 2755.
(21) Freche, P.; Grenier-Loustalot, M. F.; Metras, F. *Makromol. Chem.* **1983**, *184*, 5691.
(22) Roedel, M. J. *J. Am. Chem. Soc.* **1953**, *75*, 6110.
(23) Willbourn, A. H. *J. Polym. Sci.* **1959**, *34*, 569.
(24) Foster, G.; MacRury, T.; Hamielec, A. In "Liquid Chromatography of Polymers and Related Materials"; Marcel Dekker: New York, 1980; Vol. 13, p 143.
(25) Hert, M.; Strazielle, C. *Makromol. Chem.* **1983**, *184*, 135.
(26) Rault, J. *J. Phys., Lett. (Orsay, Fr.)* **1978**, *39*, L411.
(27) Candau, F.; Rempp, P.; Benoit, H. *Macromolecules* **1972**, *5*, 627. Candau, F.; Strazielle, C.; Benoit, H. *Makromol. Chem.* **1972**, *165*, 1.
(28) Thurmond, C.; Zimm, B. *J. Polym. Sci.* **1952**, *8*, 477.
(29) Nagasubramanian, K.; Saito, O.; Graessley, W. *J. Polym. Sci., Part A-2* **1969**, *7*, 1955.
(30) Bohdaneckŷ, M. *Macromolecules* **1977**, *10* (5), 971.
(31) Yamakawa, H. "Modern Theory of Polymer Solutions"; Wiley: New York, 1971.

Structure of Peroxy Radicals Trapped in Irradiated Isotactic Polypropylene and Molecular Disorder of the Polymer Chain, Related with Hydrogen Abstraction Reaction of the Radicals

Shigetaka Shimada, Yasurō Hori, and Hisatsugu Kashiwabara*

Nagoya Institute of Technology, Gokiso-cho, Showa-ku, Nagoya 466, Japan.
Received June 11, 1984

ABSTRACT: The conformational structure of peroxy radicals and the molecular disorder of a polymer chain in elongated isotactic polypropylene with a stretch ratio of 6 are determined from the angular dependences of the ESR spectra, which can be simulated from the calculated spectra of the partially oriented paramagnetic centers. The internal rotation angle which represents the orientation of the O–O group around the C–O bond with respect to the adjacent C–C bond, $\phi_m = -103° \pm 5°$, and the degree of orientation, $f_m = 0.536$, are estimated for mobile peroxy radicals, which decay substantially at room temperature. In addition, the internal rotation angle, $\phi_r = 55.5° \pm 1.5°$, and the degree of orientation, $f_r = 0.968$, are determined for rigid peroxy radicals, which are very stable at room temperature. The values of $\phi_m = -103°$ and $\phi_r = 55.5°$ are close to −120° and 60°, corresponding to skew and gauche conformations, respectively. The high degree of orientation, $f_r = 0.968$, is in good agreement with that of the polymer chain in crystalline regions, 0.93, obtained by X-ray diffraction. It is concluded that the mobile peroxy radicals are trapped at disordered sites in the crystalline regions, although the rigid peroxy radicals are at highly ordered sites in the same region. The reactivity of the interchain hydrogen abstraction of the mobile peroxy radicals is discussed in comparison with the rigid peroxy radicals on the basis of their conformational structures and the molecular orientations.

Introduction

Spin-label and spin-probe techniques have been developed to study the structure and dynamic behavior of polymer chains at a particular site or a particular region. We have undertaken ESR studies of much smaller spin labels, for example, alkyl radicals and peroxy radicals[1] bonded to the polymer chain. The small labels are more desirable for the study of the polymer properties than the large spin labels commonly used.

In this report, the conformational structure of peroxy radicals in isotactic polypropylene and the molecular disorder of the polymer chain are discussed on the basis of the angular dependences of the ESR spectra.

One of the purposes of the present study is to contribute to the investigation of the reaction mechanism of peroxy radicals. Eda et al.[2] and Hori et al.[3] found that the ESR spectra of peroxy radicals trapped in irradiated isotactic polypropylene are composed of two spectra arising from chemically identical peroxy radicals having different mobilities. Hori et al.[3] recently suggested very interesting conclusions: (1) The mobile peroxy radicals are trapped in crystalline regions and decay by a diffusion controlled mechanism. (2) The main mechanism is the intermolecular hydrogen abstraction by the peroxy radicals. (3) The rigid peroxy radicals are stable and the quantity of the radicals decreases with reaction temperature.

We raise two questions: Why are the mobilities of the two kinds of peroxy radicals trapped in the crystalline sites different and why do the mobile peroxy radicals abstract hydrogen intermolecularly.[3] In order to answer these questions, one must acquire a knowledge of the surrounding conditions of the peroxy radicals, for instance, the molecular orientations of the polymer chain and the conformational structures of the radicals.

Another purpose in the present article is to find a simple method for the determination of orientations in polymer materials composed of more than two different regions, the amorphous, pseudocrystalline, and crystalline, by a spin-label technique. These orientations have generally been determined by X-ray diffraction, birefringence, and sonic absorption measurements and combining them. For example, we can estimate the orientation in the region with a knowledge of the sample crystallinity and the corresponding orientation function for the crystalline region.[4] However, a shortcoming of the indirect method is that the estimated value may be subject to cumulative errors. The direct spin-label method may offer some distinct advantages for the study of local molecular orientations in the polymer sample, such as the orientations of the amorphous and crystalline regions, the interior and terminal portions of the polymer chains and the molecularly disordered regions, by introducing spin labels into these regions. An ESR method for the determination of orientations in the amorphous region by using $C_2F_4^-$ radicals has been published.[5]

In this paper, we compare the degree of orientation of the peroxy radicals in the crystalline region with that of polymer chains in the same region, obtained by X-ray diffraction measurement, and show that the ESR method is simple and effective for the determination of the ori-

0024-9297/85/2218-0170$01.50/0